

***Supporting Information:***

**Thermoresponsive plasmonic core-satellite nanostructures  
with reversible, temperature sensitive, optical properties**

Fei Han,<sup>1</sup> S.R. C. Vivekchand,<sup>1,2,3</sup> Alexander H. Soeriyadi,<sup>1,2,3</sup> Yuanhui Zheng,<sup>1,2,3</sup> J. Justin Gooding<sup>1,2,3,\*</sup>

<sup>1</sup>School of Chemistry, The University of New South Wales, Sydney, New South Wales 2052, Australia

<sup>2</sup>Australian Centre for NanoMedicine, The University of New South Wales, Sydney, New South Wales 2052, Australia

<sup>3</sup>ARC Center of Excellence in Convergent Bio-Nano Science and Technology, The University of New South Wales, Sydney, New South Wales 2052, Australia

\*corresponding author: [justin.gooding@unsw.edu.au](mailto:justin.gooding@unsw.edu.au)

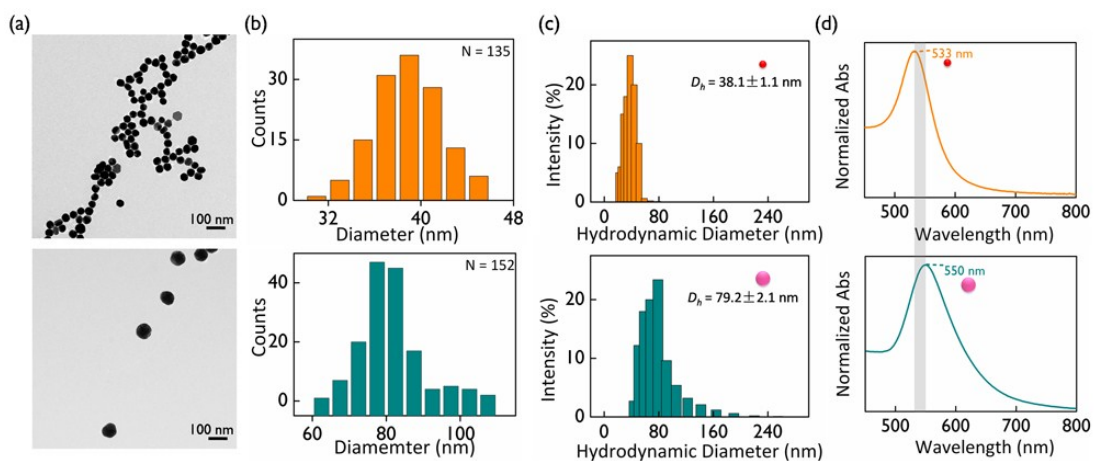


**Figure S1. ‘Satellite’ and ‘Core’ nanoparticles.** AuNP<sub>40 nm</sub> (top panel); AuNP<sub>80 nm</sub> (bottom panel). (a) TEM images; (b) The TEM image-based statistical analysis (processed by automated image analysis via ImageJ); (c) The DLS data; (d) The UV-Vis spectra.

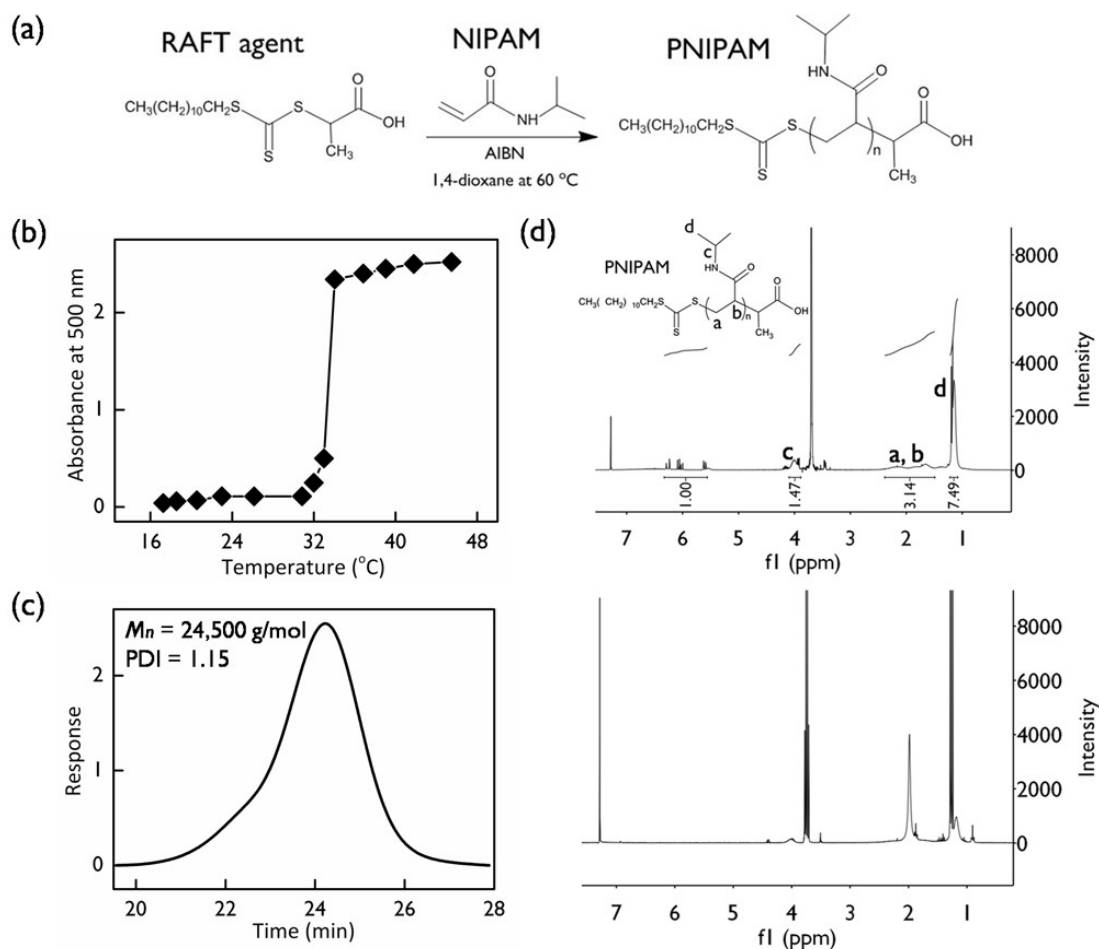


**Figure S2. Thermoresponsive polymer synthesis and characterization.** (a) Schematic illustration of poly(*N*-isopropylacrylamide) (pNIPAM) synthesis via RAFT polymerization. (b) Thermal profile (2 °C/min) of pNIPAM in Milli-Q water solution as probed by UV-Vis ( $\lambda = 500$  nm, [pNIPAM] = 5.0 mg/mL). The lower critical solution temperature (LCST) of pNIPAM is around 32 °C. At temperatures below the LCST, and the polymer chains exist as coils in water due to hydrogen bonding of amide groups with water. At temperatures above the LCST, it is generally considered that the hydrogen bonding of water with the amide groups (hydrophilic) is interrupted. Thus, hydrophobic interactions between the hydrophobic backbone and the isopropyl groups (hydrophobic) dominate, and the polymer conformation changes from linear, flexible chains to collapsed globules. Therefore, the system undergoes a hydrophilic (coil) to hydrophobic (globule) transition which lead to a cloudy solution and increase in absorbance.<sup>[1, 2]</sup> (c) GPC traces of the pNIPAM. The number-average molecular weight ( $M_n$ ) and molecular weight distribution (PDI =  $M_w/M_n$ ) were measured by GPC. The polymer shows a narrow polymer distribution (PDI = 1.15) with molecular weight of 24,500 g/mol. (d) The  $^1\text{H}$ NMR spectra and peak labels for (top panel) before purification; (bottom panel) after purification. The NMR spectrum (top panel) shows that the characteristic signals of pNIPAM at c) 3.98 and d) 1.12 ppm representing methyne and methyl protons on isopropyl groups were observed, which verify the successful synthesis of pNIPAM. The NMR spectrum in the bottom panel shows that the disappearance of the signal peaks at 5.5-6.5 represents the complete removal of the monomer. The

theoretical molecular weight was calculated according to the equation,<sup>[3]</sup>  $M_n(\text{theo}) = M_M \times \text{conv.} \times [M]_0 / [\text{RAFT agent}]_0 + M_{\text{RAFT agent}}$  where  $M_n(\text{theo})$  (= 25,000 g/mol) is the theoretically calculated molecular weight of the polymer,  $M_M$  is the molecular weight of the monomer, conv. (= 73%) is monomer conversion as determined by <sup>1</sup>HNMR spectroscopy,  $[M]_0$  and  $[\text{RAFT agent}]_0$  are the concentration of the monomer and the concentration of the RAFT agent,  $M_{\text{RAFT agent}}$  is the molecular weight of the RAFT agent. (Experimental conditions:  $[\text{NIPAM}]_0 / [\text{RAFT agent}]_0 / [\text{AIBN}]_0 = 300/1/0.2$ ).

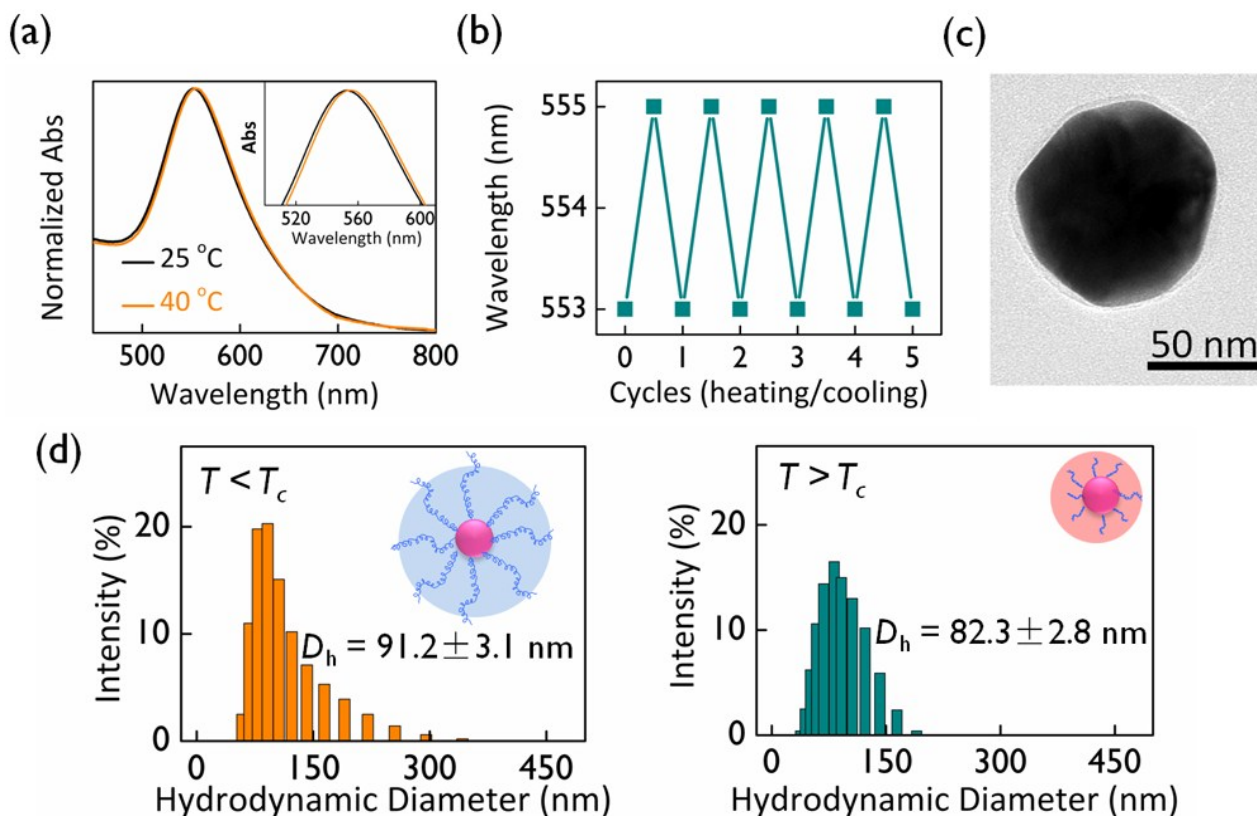


**Figure S3. Optical, structural properties and TEM images of the pNIPAM@AuNP<sub>80 nm</sub>.** (a) UV-Vis spectra; (b) reversibility measurements; (c) TEM images; (d) DLS data. DLS studies of pNIPAM@AuNP<sub>80 nm</sub> at 0.18 mM mL<sup>-1</sup> in aqueous media were conducted. The size measurements were conducted in a cuvette with the temperature changing from 25 °C to 40 °C. Samples were allowed to equilibrate for 5 min after reaching the desired temperature before measurement. It is evident that the LCST affects the pNIPAM length<sup>[4]</sup> thereby inducing the reduction in size from 91 nm to 82 nm.

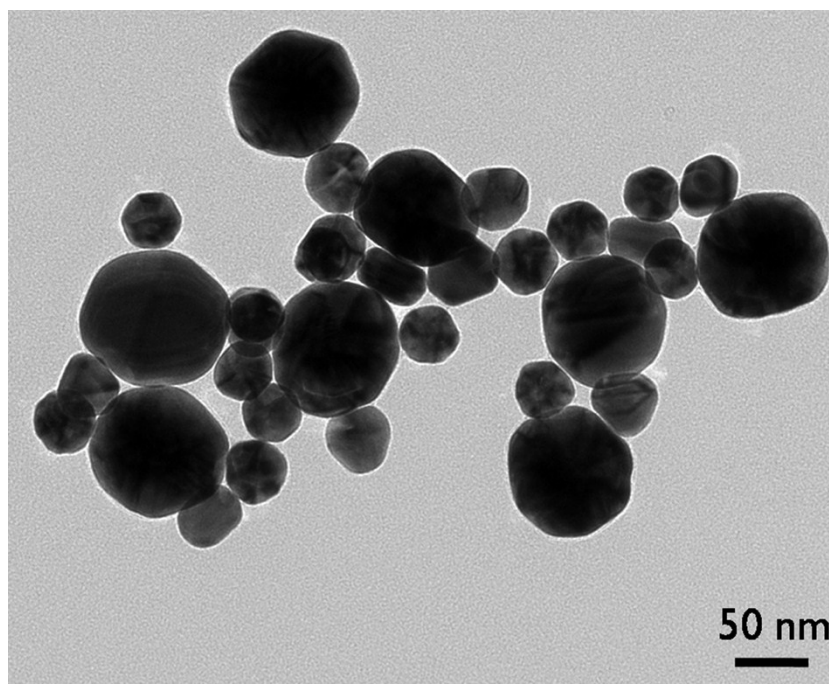


**Figure S4.** TEM images of core<sub>80 nm</sub>-satellite<sub>40 nm</sub> nanostructures at a lower number ratio of satellite: core (20: 1). Reaction conditions: the 2.5  $\mu\text{L}$ , 1% MPTMS ethanol solution ( $[\text{MPTMS}]: [\text{AuNP}] = 10^5: 1$ ) was added into the 100  $\mu\text{L}$  pNIPAM@AuNP<sub>80 nm</sub> to change the end group of the pNIPAM from -COOH to -SH. After 1 h agitation at 900 rpm, the excess MPTMS was removed by centrifugation at least 2 times at 3500 rpm in 20 min. the resultant was redispersed in the Milli-Q water for 100  $\mu\text{L}$ . Then 10  $\mu\text{L}$  Tween 20 (2.5%) (surfactant) and 25  $\mu\text{L}$  NaCl (0.2 M) were added into the 150  $\mu\text{L}$  AuNP<sub>40 nm</sub> solution. After gently shaking, the 100  $\mu\text{L}$  pNIPAM-SH@AuNP<sub>80 nm</sub> solutions were added into the satellites solution dropwise. After overnight agitation at 900 rpm, the unreacted satellites, NaCl and Tween 20 were removed by the centrifugation at least 3 times at 3500 rpm in 20 min. The resultant was diluted to the 100  $\mu\text{L}$  in the Milli-Q water.

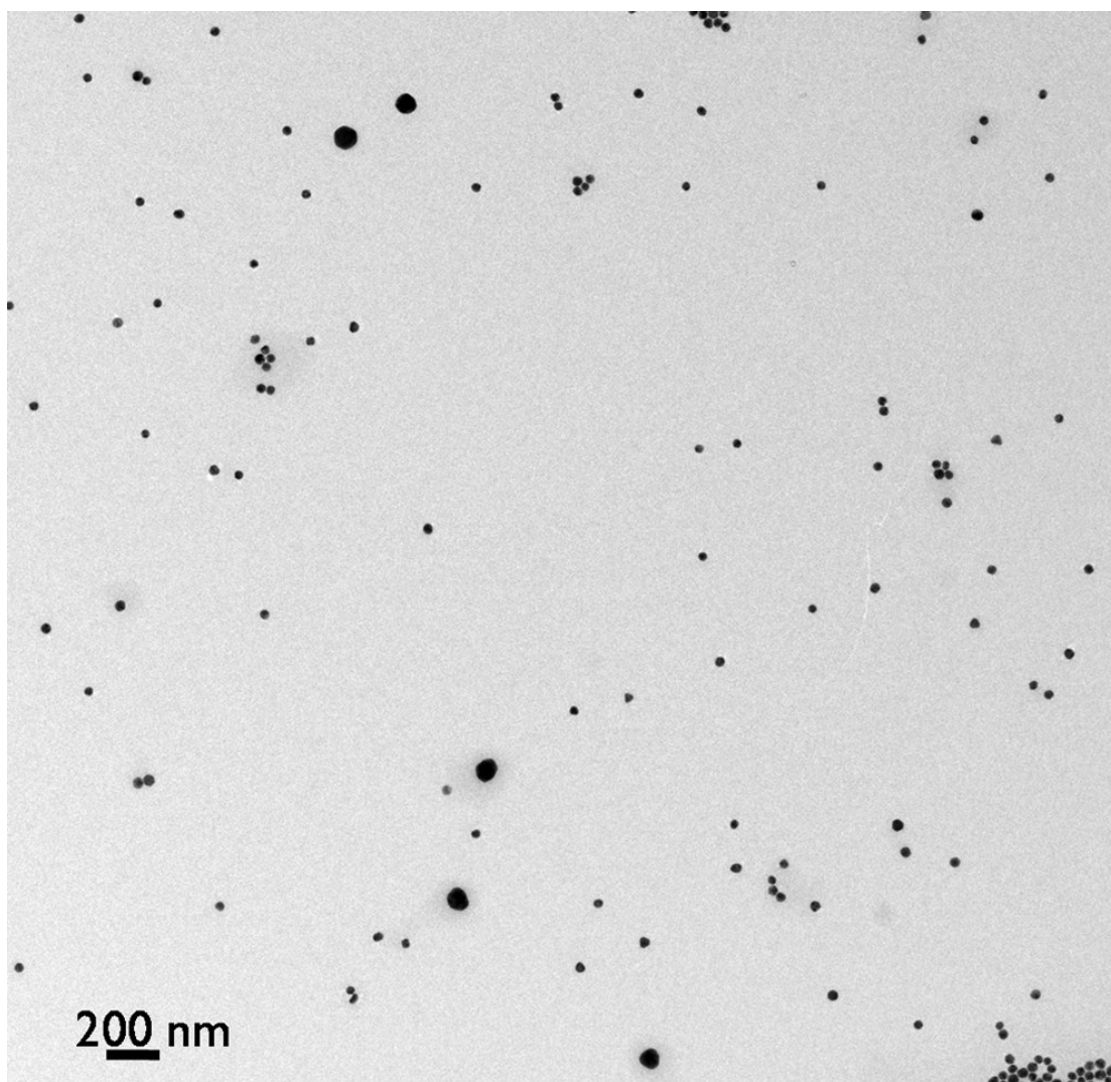


**Figure S5.** TEM images of randomly dispersed gold nanoparticles (AuNP<sub>80 nm</sub> and AuNP<sub>40 nm</sub>).

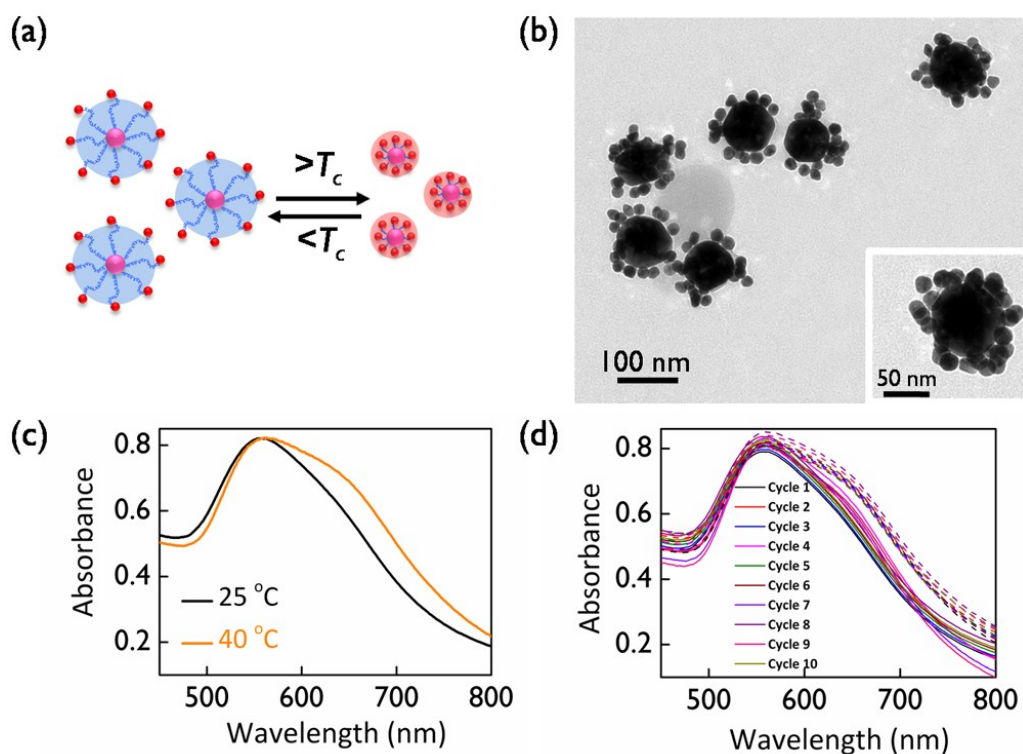


**Figure S6.** The thermoresponsive tuning of plasmonic properties of core<sub>80 nm</sub>-satellite<sub>20 nm</sub> nanostructures: (a) Schematic illustrating the responsive behavior of the core<sub>80 nm</sub>-satellite<sub>20 nm</sub> nanostructures; (b) TEM images; (c) The UV-Vis spectra of the core<sub>80 nm</sub>-satellite<sub>20 nm</sub> nanostructure at 25 °C and 40 °C; (d) The reversibility measurements during 10 cycles of repeated heating (at 40 °C) and cooling (at 25 °C).

The excess number ratio of 1:200 (core<sub>80 nm</sub>: satellite<sub>20 nm</sub>) was chosen to ensure there was sufficient coverage of satellites on each core and hence the probability of formation of aggregates was lowered. The TEM images of the core<sub>80 nm</sub>-satellite<sub>20 nm</sub> nanostructures with the different numbers of satellites on each core were shown in Figure S5b. The plasmon absorbance maxima of satellite<sub>20 nm</sub> were found to be at 525 nm. Core<sub>80 nm</sub>-satellite<sub>20 nm</sub> nanostructures exhibit a shoulder at ~600 nm at 25 °C; while a shoulder at longer wavelengths ~650 nm appeared at 40 °C. It demonstrates that the decrease in distance among the core<sub>80 nm</sub> and satellites<sub>20 nm</sub> gives rise to the surface plasmon coupling band abruptly red-shifting and becoming more evident. Compared to the core<sub>80 nm</sub>-satellite<sub>40 nm</sub> nanostructures, the core<sub>80 nm</sub>-satellite<sub>20 nm</sub> nanostructures generate relatively smaller peak shifts and the plasmon coupling among the core and satellites becomes weaker. It is clear that the increase in the diameter of satellites will lead to the more red shift and stronger coupling among the core and satellites.<sup>[5]</sup>

Reaction conditions: the 1.5  $\mu\text{L}$ , 1% MPTMS ethanol solution ( $[\text{MPTMS}]: [\text{AuNP}] = 10^5: 1$ ) was added into the 100  $\mu\text{L}$  pNIPAM@AuNP<sub>80 nm</sub> to change the end group of the pNIPAM from -COOH to -SH. After 1 h agitation at 900 rpm, the excess MPTMS was removed by centrifugation at least 2 times at 3500 rpm in 20 min. the resultant was redispersed in the Milli-Q water for 100  $\mu\text{L}$ . Then 10  $\mu\text{L}$  Tween 20 (2.5%) (surfactant) and 25  $\mu\text{L}$  NaCl (0.2



M) were added into the 315  $\mu\text{L}$  AuNP<sub>20 nm</sub> solution. After gently shaking, the 100  $\mu\text{L}$  pNIPAM-SH@AuNP<sub>80 nm</sub> solutions were added into the satellites solution dropwise. After overnight agitation at 900 rpm, the unreacted satellites, NaCl and Tween 20 were removed by the centrifugation at least 3 times at 3500 rpm in 20 min. The resultant was diluted to the 100  $\mu\text{L}$  in the Milli-Q water.

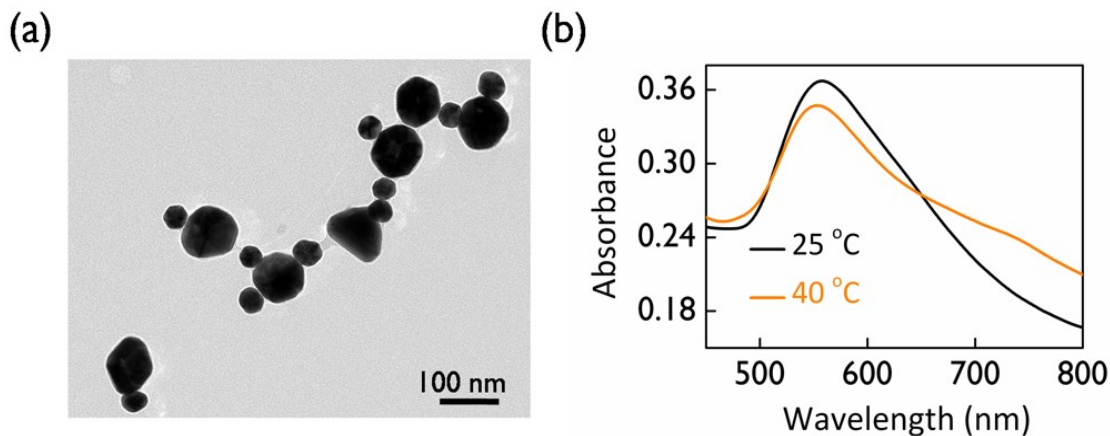


**Figure S7.** Core<sub>80 nm</sub>-satellite<sub>40 nm</sub> nanostructures with the reaction conditions: 1  $\mu\text{L}$ , 1% MPTMS ethanol solution ([MPTMS]: [AuNP] = 10<sup>5</sup>: 1): (a) TEM images, and (b) The UV-Vis spectra.

Decreasing the amount of the MPTMS gives rise to a reduction in the possibility of converting the end group of the pNIPAM from -COOH into -SH, therefore leading to the reduction of numbers of satellites per core. The UV-Vis spectra show that the less numbers of satellites per core generates a shoulder at  $T > T_c$ , i.e. coupling among the core and satellites will be weakened because of the insufficient numbers of satellites per core.<sup>[6]</sup> Therefore, the amount of MPTMS should be optimized.

Reaction conditions: the 1  $\mu\text{L}$ , 1% MPTMS ethanol solution ([MPTMS]: [AuNP] = 10<sup>5</sup>: 1) was added into the 100  $\mu\text{L}$  pNIPAM@AuNP<sub>80 nm</sub> to change the end group of the pNIPAM from -COOH to -SH. After 1 h agitation at 900 rpm, the excess MPTMS was removed by centrifugation at least 2 times at 3500 rpm in 20 min. the resultant was redispersed in the Milli-Q water for 100  $\mu\text{L}$ . Then 10  $\mu\text{L}$  Tween 20 (2.5%) (surfactant) and 25  $\mu\text{L}$  NaCl (0.2 M) were added into the 365  $\mu\text{L}$  AuNP<sub>40 nm</sub> solution. After gently shaking, the 100  $\mu\text{L}$  pNIPAM-SH@AuNP<sub>80 nm</sub> solutions were added into the satellites solution dropwise. After overnight agitation at 900 rpm, the unreacted satellites, NaCl and Tween 20 were removed by the sedimentation. The resultant was diluted to the 100  $\mu\text{L}$  in the Milli-Q water.

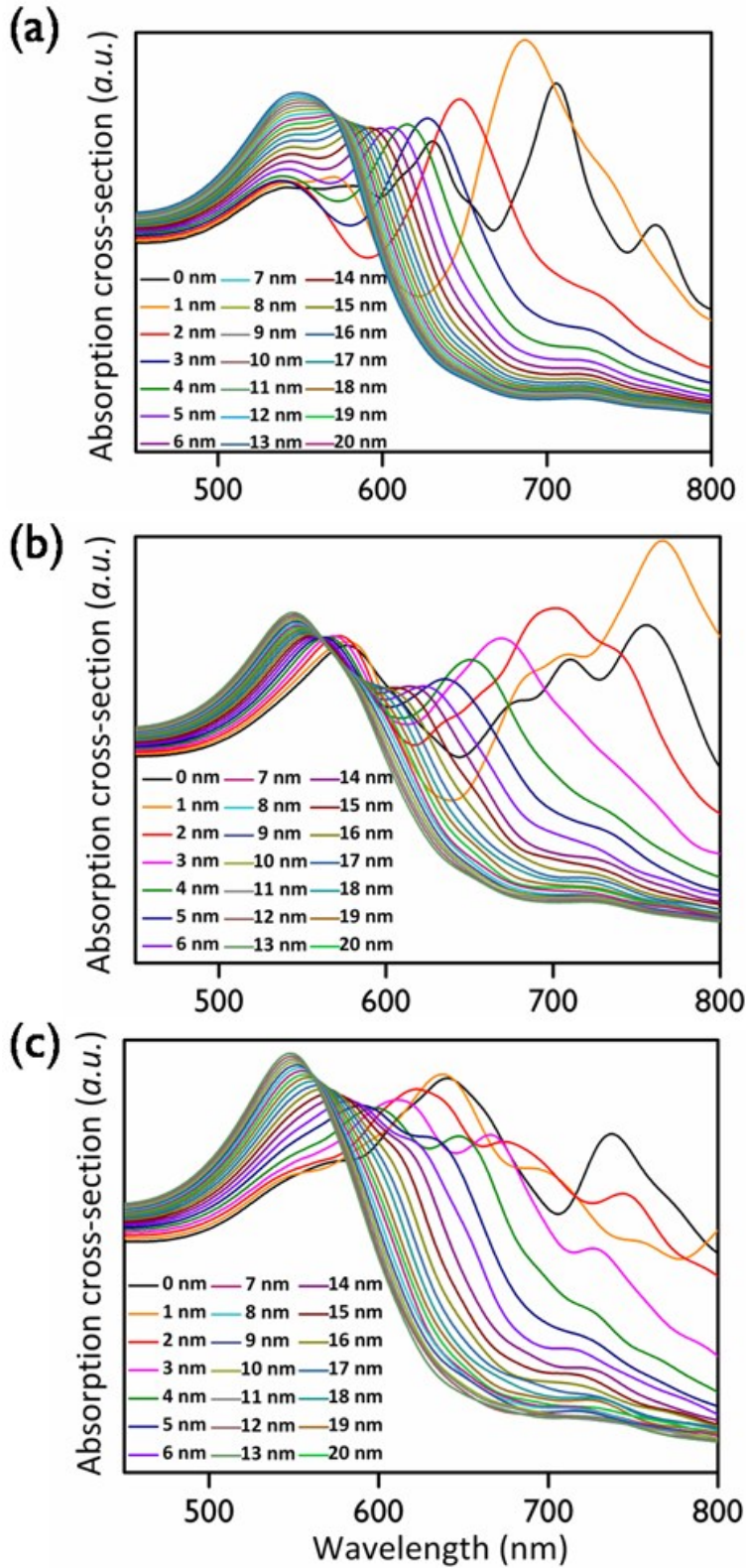


**Figure S8.** Simulated absorption spectra as a function of gap distance ranging from 0 to 20 nm. (a) 6 satellites; (b) 10 satellites (symmetry); (c) 10 satellites (off-angle symmetry) where two of the satellites are located in the  $z$  direction with one in front of the  $xy$  plane and one behind the  $xy$  plane.

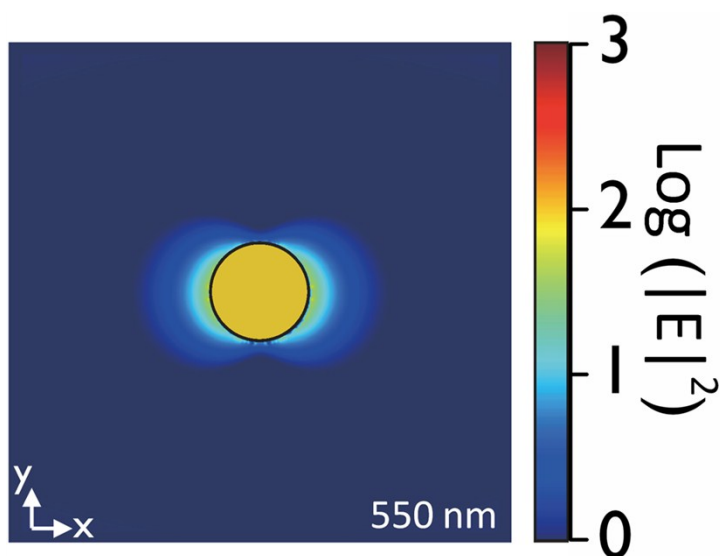


**Figure S9.** Electric field intensity profile in the xy plane for the AuNP<sub>80 nm</sub>.

## References

- [1] R. Liu, M. Fraylich, B. R. Saunders, *Colloid Polym. Sci.* **2009**, *287*, 627-643;
- [2] K. Jain, R. Vedarajan, M. Watanabe, M. Ishikiriyama, N. Matsumi, *Polym. Chem.* **2015**, *6*, 6819-6825.
- [3] H. Li, A. P. Bapat, M. Li, B. S. Sumerlin, *Polym. Chem.* **2011**, *2*, 323-327.
- [4] J. Liu, A. Li, J. Tang, R. Wang, N. Kong, T. P. Davis, *Chem. Commun.* **2012**, *48*, 4680-4682.
- [5] B. M. Ross, J. R. Waldeisen, T. Wang, L. P. Lee, *Appl. Phys. Lett.* **2009**, *95*, 193112.
- [6] J. H. Yoon, Y. Zhou, M. G. Blaber, G. C. Schatz, S. Yoon, *J. Phys. Chem. Lett.* **2013**, *4*, 1371-1378.